Journal of Organometallic Chemistry 751 (2014) 534–540

Contents lists available at ScienceDirect

Journal of Organometallic Chemistry

journal homepage: www.elsevier.com/locate/jorganchem

Metal and halogen dependence of the rate effect in hydroamination/cyclization of unactivated aminoalkenes: Synthesis, characterization, and catalytic rates of CCC-NHC hafnium and zirconium pincer complexes

Wesley D. Clark [a], Joon Cho [b], Henry U. Valle [a], T. Keith Hollis [a,*], Edward J. Valente [c]

[a] Department of Chemistry, Mississippi State University, Mississippi State, MS 39762, United States
[b] Department of Chemistry and Biochemistry, The University of Mississippi, University, MS 38677, United States
[c] Department of Chemistry and Biochemistry, University of Portland Diffraction Facility, University of Portland, Portland, OR 97203, United States

ARTICLE INFO

Article history:
Received 1 June 2013
Received in revised form
1 November 2013
Accepted 1 November 2013

Keywords:
N-Heterocyclic carbene
CCC-NHC pincer complex
Hydroamination
Homogenous catalysis
Pyrrolidines
Piperidines

ABSTRACT

1,3-Bis(3′-butylimidazol-1′-yl)benzene dibromide (**2b**) or 1,3-bis(3′-butylimidazol-1′-yl)benzene dichloride (**2c**) was reacted with a stoichiometric amount of $Zr(NMe_2)_4$ or $Hf(NMe_2)_4$ yielding four new early transition metal CCC-*N*-heterocylic carbene (CCC-NHC) pincer complexes. Two of the CCC-NHC pincer complexes were synthesized via a new methodology, which allowed for a room temperature reaction, shorter reaction times, and slightly less $Zr(NMe_2)_4$ or $Hf(NMe_2)_4$. The molecular structure of 2-(1,3-bis-3′-butylimidazol-1′-yl-2′-ylidene)phenylene)(dimethylamido)(dibromo)zirconium(IV) (**3b**) was determined by X-ray crystallography. The complexes were evaluated for hydroamination/cyclization of unactivated aminoalkenes yielding pyrrolidines or piperidines. The hydroamination/cyclization rates were dependent upon the halogen or the metal in the complex. The complexes with iodide ligands gave the fastest hydroamination/cyclization rates (I > Br > Cl). The Zr complexes provided faster hydroamination/cyclization rates than the Hf analogs. Use of CCC-NHC ZrI_3 complex **5** enhanced the rate of reaction.

1. Introduction

Pyrrolidines and piperidines are important classes of *N*-heterocycles present in many natural products, biologically active molecules, and pharmaceuticals [1]. Hydroamination/cyclization of unactivated aminoalkenes is an atom economical pathway to these molecules [2]. However, a catalyst is required due to a high activation barrier from electrostatic repulsion of the olefin π-bond and the amine lone pair [3]. Amidate, ureate, and trans-disubstituted cyclam early transition metal complexes were reportedly utilized in the catalytic hydroamination/cyclization of aminoalkenes and the asymmetric synthesis of substituted morpholines and piperazines [4]. A series of chiral Zr based catalysts were recently disclosed that enantioselectively catalyzed the formation of 5, 6, and 7 membered *N*-heterocycles [5]. Yttrium, scandium, titanium, and organolanthanide hydroamination/cyclization catalysts have also been reported [6]. Furthermore, a wide variety of hydroamination/cyclization catalysts have been reported incorporating chiral or achiral ligands, early and late transition metals, rare earth metals, and often halogen ligands [4–6,7]. However, the effects of halogen ligands have received little attention [8]. Understanding the way halogen ligands impact hydroamination/cyclization rates may lead to improved catalysts.

Over the past two decades, NHC complexes have become useful catalytic reagents in many reactions [9]. NHCs are stronger σ donors and dissociate less readily than their phosphine counterparts [10]. These properties have lead to many applications in catalysis, solar cells, and biomedical fields [9a,11]. Additional stability can be obtained through the use of chelating, pincer type ligands [12]. Due to the lack of need to activate the nitrogen in the pyridylene moiety, many CNC–NHC pincer complexes have been reported [7s,11c,13]. However, fewer examples of CCC-NHC pincer complexes have been reported [11b,14]. We recently disclosed the synthesis and hydroamination/cyclization activity of 2-(1,3-bis(3′-butyl-imidazol-2′-ylidene)phenylene)(dimethylamido)diiodozirconium(IV) (**3a**), and 2-(1,3-bis(3′-butyl-imidazol-2′-ylidene)phenylene)(dimethylamido)diiodohafnium(IV) (**4a**) [14b,c]. Herein, we report the expansion

* Corresponding author.
E-mail addresses: khollis@chemistry.msstate.edu, tkhollis@gmail.com (T.K. Hollis).

0022-328X/$ – see front matter © 2013 Elsevier B.V. All rights reserved.
http://dx.doi.org/10.1016/j.jorganchem.2013.11.001

of this methodology to form the 2-(1,3-bis(3′-butyl-imidazol-2′-ylidene)phenylene)(dimethylamido)dibromozirconium(IV) (**3b**), 2-(1,3-bis(3′-butyl-imidazol-2′-ylidene)phenylene)(dimethylamido) dichlorozirconium(IV) (**3c**), 2-(1,3-bis(3′-butyl-imidazol-2′-ylidene)phenylene)(dimethylamido)dibromohafnium(IV) (**4b**), and 2-(1,3-bis(3′-butyl-imidazol-2′-ylidene)phenylene)(dimethylamido) dichlorohafnium(IV) (**4c**). A large rate effect was observed in hydroamination/cyclization of unactivated aminoalkenes, which was dependent upon the halogen ligands or metal involved.

2. Results and discussion

2.1. Synthesis and characterization

1,3-Dibromobenzene and imidazole were heated in the presence of CuO, K_2CO_3, and DMSO yielding 1,3-bis(imidazol-1′-yl) benzene (**1**) according to the literature procedure (Scheme 1 [14c]). The previously reported alkylation of 1,3-bis(imidazol-1′-yl)benzene (**1**) with 1-iodobutane was expanded to 1-bromobutane or 1-chlorobutane yielding imidazolium salts **2a**–**c** in excellent yields [14c].

CCC-NHC pincer complexes **3b** and **4b** were obtained by heating imidazolium salts **2b** with $Zr(NMe_2)_4$ or $Hf(NMe_2)_4$ and isolated as analytically pure crystalline solids after filtration and drying under reduced pressure. A satisfactory elemental analysis for complex **3c** was obtained after synthesizing the complex using more polar solvents (CH_2Cl_2 and THF vs toluene), slightly less $Zr(NMe_2)_4$ (1.0 eq vs 1.1 eq) and lower temperatures (room temperature vs 160 °C). Increased solubility of imidazolium salt **2c** in the higher polarity solvents presumably allows lower reaction temperatures. High solubility of complex **3c** in the more polar solvents hampered efficient isolation of the complex. The yields of complexes **3a**–**c** and **4a**–**c** vary significantly, and reflect different concentrations and solubilities of complexes **3a**–**c** and **4a**–**c** in room temperature toluene. A satisfactory elemental analysis was not obtained for complex **4c** and this result is presumably due to extreme sensitivity to proton sources; in particular, humid air. The elemental analysis results of complex **4c** are consistent with partial hydrolysis of complex **4c**. The loss of imidazolium proton signals around δ 11.4–11.6 and only 4 signals in the aromatic region in the ^{1}H NMR spectra were consistent with the formation of CCC-NHC pincer complexes. The appearance of a resonance at δ 192–200 in the ^{13}C NMR spectra was also consistent with the formation of CCC-NHC pincer complexes. The ^{1}H and ^{13}C NMR spectra of pincer complexes **3b**, **c**, **4b**, and **c** were consistent with previously reported and structurally characterized pincer complexes **3a** and **4a** [14b,c].

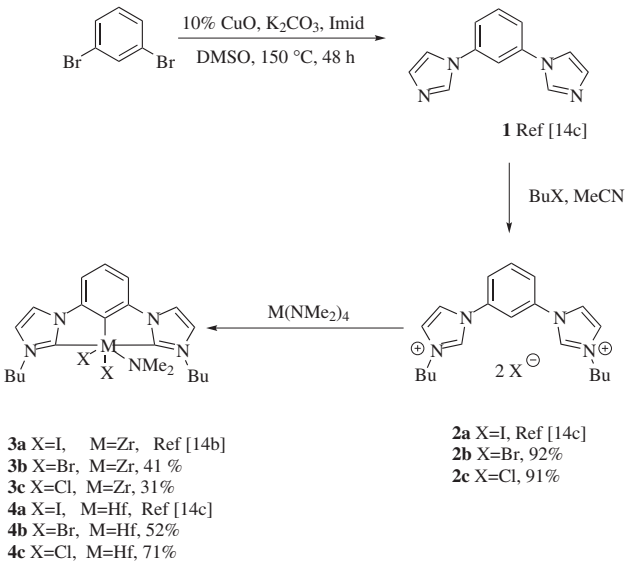

Scheme 1. Synthesis of 1,3-bis(imidazol-1′-yl)benzene **1**, imidazolium salts **2a**–**c**, and CCC-NHC pincer complexes **3a**–**c** and **4a**–**c**.

2.2. X-ray crystallography

During the synthesis of dibromo Zr complex **3b**, slow cooling of the reaction mixture yielded crystals suitable for single crystal X-ray diffraction. An ORTEP® illustration of the molecular structure of dibromo Zr complex **3b** is shown in Fig. 1. The coordination sphere around Zr is a distorted octahedron with the amido group in an axial position. The Zr–$C_{carbene}$ bond lengths are very similar to the previously published diiodo analog **3a** (Δ = 0.015 Å, [14b]). However, the Zr–$C_{carbene}$ bonds in dibromo Zr complex **3b** are longer than the Zr–$C_{carbene}$ bond in Cavell's Zr hydrocarbyl bis(phosphoranimino) pincer carbene complex (Δ = 0.139 Å and 0.1668 Å [15],). The Zr–C7 bond in the dibromo Zr complex **3a** (ZrI1 vs. ZrI2, Δ = 0.1607 Å longer than in the diiodo Zr complex **3a** [14b]. The Zr–Br1 bond is slightly longer than the Zr–Br2 bond in dibromo Zr complex **3b**, an effect that is likely due to the stronger trans influence of the amido ligand (Δ = 0.0862 Å). This effect was also observed in the diiodo Zr complex **3a** (ZrI1 vs. ZrI2, Δ = 0.1607 Å [14b],). The Zr–N25 bond in dibromo Zr complex **3b** is only slightly longer than in the diiodo Zr complex **3a** (Δ = 0.0337 Å [14b],). However, the Zr–N25 bond is shorter than all Zr–N bonds found in two Zr complexes of a tacn-derived amido ligand [16].

2.3. Hydroamination/cyclization catalysis

2.3.1. Effect of precatalyst loading

Standard substrate, 2,2-diphenylpent-4-ene-1-amine, was used to assay the precatalysts. Quantitative conversions (>98%) were observed in precatalyst loading experiments with 5 mol % diiodo Zr complex **3a** after 50 min of heating (Table 1, entry 1 [14b],). The dibromo Zr complex **3b** required much longer reaction times (10 h vs. 50 min) to achieve the same conversion (>98%, entry 1). Despite even longer reaction times (32 h vs 2 h, entry 2), reactions using 2.5 mol % dibromo Zr complex **3b** did not reach quantitative conversion. Good conversions were still achieved even at 1 mol % precatalyst loading but required extended reaction times. Reactions using dibromo Zr complex **3b** required much longer reaction times. For both complexes, good conversions were achieved at 5, 2.5 and

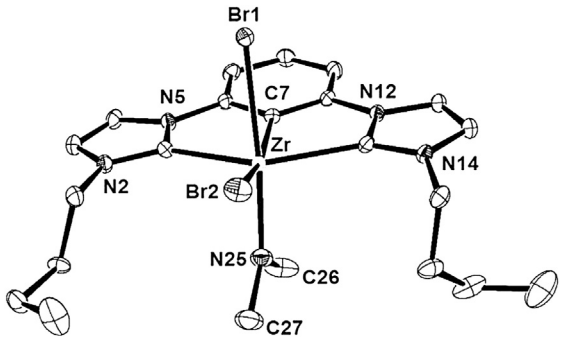

Fig. 1. ORTEP diagram of dibromo Zr complex **3b** with thermal ellipsoids at 50% confidence level. Hydrogens were omitted for clarity. Only one conformer of the disordered butyl chain is shown. Selected bond lengths (Å) and angles (°): Zr–C1 2.347(2), Zr–C7 2.315(2), Zr–C13 2.3748(19), Zr–Br1 2.7535(3), Zr–Br2 2.6673(3), Zr–N25 2.0197(18), C1–Zr–Br1 86.39(5), C1–Zr–N25 94.76(7).